Title:

Cortical state change by auditory deviants: a mismatch response generation mechanism in unconsciousness

Adam Hockley[1,2,3, *, ♦], Laura H Bohórquez[1,2,3], Manuel S Malmierca[1,2,3]
1 Cognitive and Auditory Neuroscience Laboratory, Institute of Neuroscience of Castilla y León (INCYL), Salamanca, Spain
2 Salamanca Institute for Biomedical Research (IBSAL), Salamanca, Spain
3 Department of Cell Biology and Pathology, Faculty of Medicine, University of Salamanca, Salamanca, Spain
♦ Senior author
* Correspondence adamhockley@usal.es

Author contributions:
Adam Hockley: Conceptualization, Methodology, Software, Formal analysis, Investigation, Writing - Original Draft, Writing – Review & Editing, Visualization, Supervision, Funding acquisition
Laura H Bohorquez: Investigation, Methodology, Writing - Original Draft, Writing – Review & Editing
Manuel S Malmierca: Conceptualization, Writing – Review & Editing, Supervision, Funding acquisition

Declaration of interests:
The authors declare no competing interests.

Acknowledgements:
This study was supported by projects PROOPI340-USAL4EXCELLENCE funded by H2020-MSCA-COFUND-2020 to AH and MSM; PID2023-148541OB-I00 funded by MCIN/AEI to MSM; Foundation Ramón Areces grant CIVP20A6616 to MSM; and Consejería de Educación, Junta de Castilla y León (SA218P23) to MSM.

Keywords:
Mismatch negativity, Up state, cortical slow oscillations, synchronised activity, anesthesia, auditory cortex, prefrontal cortex, omission, prediction error

Data Availability Statement:
Data will be made available on Zenodo and analysis code available on GitHub before publication.

ABSTRACT

Mismatch negativity is an auditory-evoked biomarker for an array of neuropsychological disorders that occurs irrespective of consciousness, yet the generation mechanisms are still debated. Cortical slow oscillations occur during sleep or anesthesia and consist of reliable changes between “Up” and “Down” phases, characterised by high and low neural activity, respectively. Here we measure electrocorticography responses in the urethane-anesthetised rat and we demonstrate that during an auditory “oddball” paradigm, deviants trigger cortical Up phase initiations. Triggering of Up phases creates a mismatch response across the cortex, and when deviants fail to trigger Up phases, no mismatch response is present. We therefore propose triggering of cortical Up phases as a mechanism for mismatch negativity generation in unconscious states.

INTRODUCTION

Cortical processing of stimuli is highly dependent on cortical state [1–3]. Two state extremes observed during sleep are characterised as the desynchronised state with rapid eye movement and the synchronised state with non-rapid eye movement [4]. During the synchronised state, cortical slow oscillations occur, consisting of reliable changes between “Up” and “Down” phases and are characterised by high and low neural activity, respectively [4–6]. Up/Down phase changes occur at a rate of 0.2-0.5 Hz and are a global event throughout the thalamus and cortex during the synchronised brain states of slow-wave sleep and deep anesthesia [7]. Slow oscillations have been recorded with a wide range of methods, from *in vitro* single cells to scalp electroencephalography [8,9]. Triggering of Up phases is a topic still under debate, but the thalamus plays a critical role. Cortical oscillations are present in the deafferented cortex [10], demonstrating that thalamocortical input is not required. However inactivation of the thalamus greatly reduces slow oscillation frequency [11–13]. Furthermore, thalamocortical activity precedes the Up phase, suggesting that the most likely role for thalamocortical activity in slow oscillations is the initiation of Up phases, hence acting as a controller of Up phase frequency [14]. External somatosensory and visual stimuli have also been shown to initiate Up phases in the cortex, with the travelling wave initiated from the relevant sensory cortex [15–17]. Urethane can be used as a model for state changes, as it induces the full spectrum of sleep cycle, including rhythmic and regular state alternations [18–20] . Under urethane anesthesia more time is spent in the synchronised state with a stronger dose [20], and clear Up and Down phases occur [21–24].

Mismatch negativity (MMN) is an evoked potentials that can be recorded in humans and is a biomarker for various neuropsychological disorders [25–28], yet the generation mechanisms are debated [29–32]. The auditory ‘oddball’ paradigm consisting of repeating standard (STD) stimuli and rare deviant stimuli (DEV) has been widely used to study MMN, along with its proposed neural correlates of stimulus-specific adaptation and prediction error in single neurons [31,33]. MMN and its neural correlates are present in sleep [34–36] and anesthesia [37–40], and neuronal stimulus-specific adaptation is even increased under certain anesthetic states [41,42]. Greater DEV responses occur in the auditory thalamus during the oddball paradigm[33,43,44], and increased

80 thalamocortical activity can trigger an Up state [14], therefore we hypothesise that DEV stimuli
81 may trigger cortical Up phases under anesthesia.
82 Here we measure electrocorticography responses in the urethane-anesthetised rat which
83 presents strong spontaneous Up/Down phases. We describe how deviant stimuli in an auditory
84 "oddball" paradigm trigger cortical Up phase initiations. Triggering of Up phases creates a
85 mismatch response (MMR) beginning in the left auditory cortex and spreading across the
86 cortex. When deviants fail to trigger Up phases, no other deviant response is present. We
87 therefore propose triggering of cortical Up phases as a mechanism for MMN generation in
88 unconscious states.
89
90 **RESULTS**
91 **Urethane induces spontaneous Up/Down phases**
92 Here, we use electrocorticography (ECoG) recordings from 6 rats with recording sites over left
93 and right auditory cortex (AC-L & AC-R) and medial prefrontal cortex (mPFC-L & mPFC-R) (Fig
94 1A). After anesthetic induction with urethane, we surgically implanted an ECoG array and
95 performed all recordings at 4-6 hours after anesthetic induction. In the absence of sensory
96 stimuli, we observed Up phases in filtered (1-150 Hz) local field potential (LFP) recordings
97 occurring coincidentally across all 6 electrodes (Fig 1B). They consisted of increased activity
98 lasting 1-3 seconds across traditional oscillatory bands, with high-frequency activity nested on
99 the Up phase (Fig 1 C&D). We demonstrate that urethane-anesthetised rats exhibit cortical
100 slow oscillations, consisting of spontaneous Up and Down phases (Fig 1 B-D), as has been
101 previously reported [21–24].
102

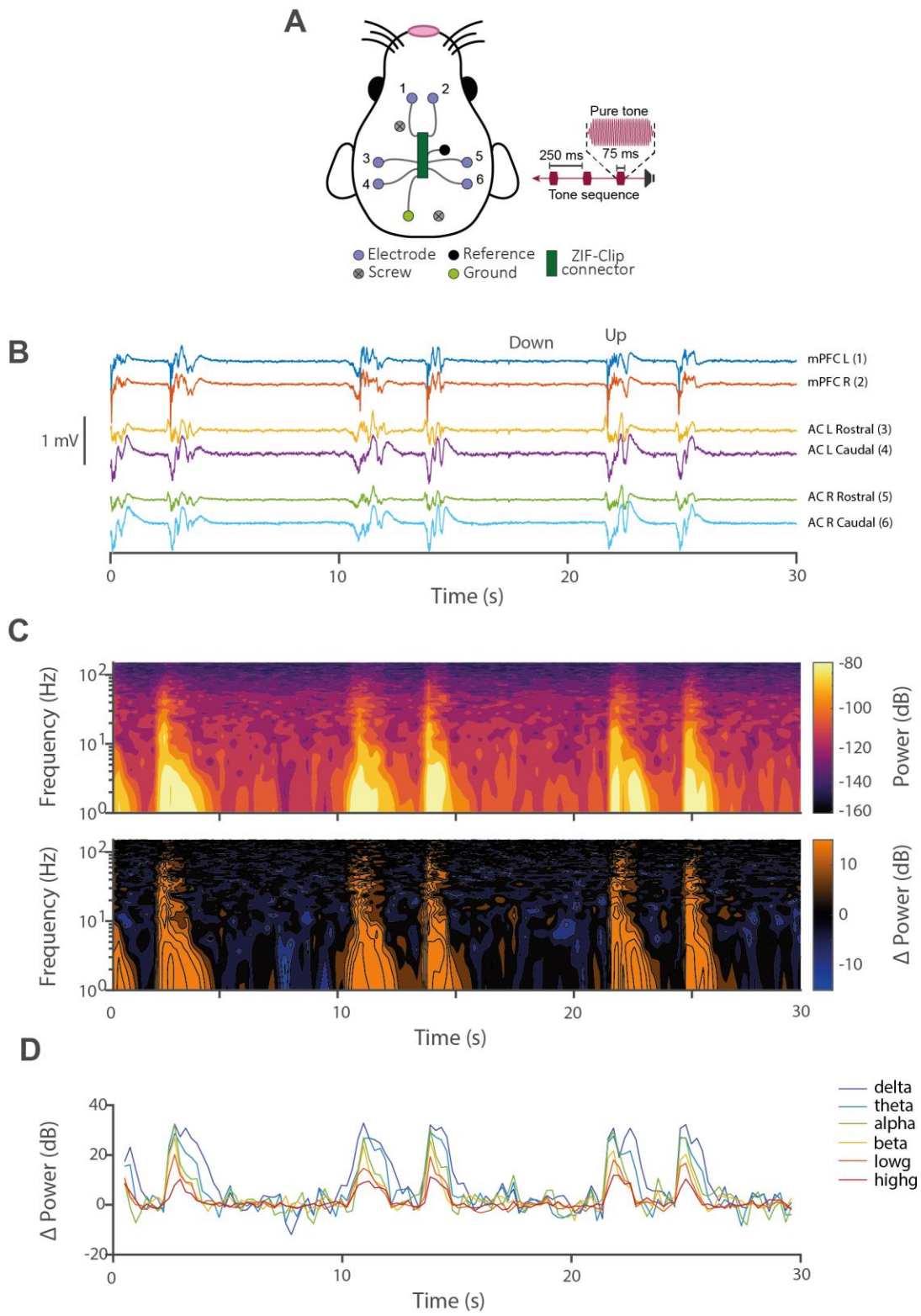

Figure 1: Spontaneous Up and Down phases in the urethane-anesthetised rat A) Schematic of the 6 recording sites, two over mPFC (1 & 2) and 2 bilaterally over AC (3 & 5 rostral; 4 & 6 caudal). **B)** Example simultaneous LFP traces from all 6 electrode sites show that Up phases are

coincidental across electrode sites. Data from 30s of silence is shown, during which cortical Up and Down phases are observed. **C)** Spontaneous cortical Up phases are associated with increased activity across oscillatory bands. Top shows spontaneous power for the LFP trace in B. Spontaneous increases occur across traditional oscillators bands and align with LFP trace peaks. Bottom shows change in power from baseline. **D)** Oscillatory power traces demonstrate coincidental increases across all power bands.

Auditory deviants trigger cortical Up phases which generate mismatch responses

To test whether the auditory oddball paradigm could trigger cortical Up phases, we presented an auditory oddball paradigm consisting of a repeating STD tone of 10 kHz and a rare DEV tone of 14.142 kHz (250 ms stimulus onset asynchrony (SOA); 6.45% DEV probability; inter-DEV interval 3 - 4.75 s; 60 dB SPL; 75 ms tones) while recording ECoG activity as in Fig 1. The inter-DEV interval of this 'oddball' paradigm is optimised for initiating slow oscillatory activity of ~0.2-0.35 Hz, approximate to the spontaneously occurring Up phase frequency. We identified Up phase initiations using negative peaks of the filtered (0.1-10 Hz) LFP traces from the mPFC-L electrode (Fig 2A). Data from the mPFC-L were used to identify Up phase initiations as this electrode had the greatest signal-to-noise ratio, but note that Up phases were coincidental across all electrode sites, as in Fig 1B. Previously spontaneous Up phases were triggered by DEVs (Fig 2A). For all 6 animals, DEV stimuli of the oddball paradigm initiated cortical Up phases, with Up phases triggered by 50%, 82%, 27%, 60%, 67% and 35% of DEVs in rats 1-6, respectively. Further, it is of note that the responses to DEVs were often long-lasting, with change in activity that lasted ~1-3 s, consistent with cortical Up phases under urethane anesthesia. The effect was highly reliable, and we quantified Up phase triggering using cross-correlation synchrony between timings Up phase initiation and DEV or STD stimuli, using an average of the STDs 2-5 stimuli before the DEV. In 5/6 animals, synchrony values for DEV-Up were greater than those for STD-Up (Fig 2B), with peak synchrony at ~200 ms. MMRs were calculated for mPFC-L and AC-L data (DEV response – STD response, for final STD only) for each presentation and these data were separated into two groups dependent on whether an Up phase was initiated on that trial (MMR-Up & MMR-noUP). In mPFC-L and AC-L, MMRs are only present when an Up phase is initiated, largely occurring in a window of 200-500 ms (Fig 2C).

These results reveal that auditory DEVs trigger cortical Up phase initiation under urethane anesthesia, generating MMRs.

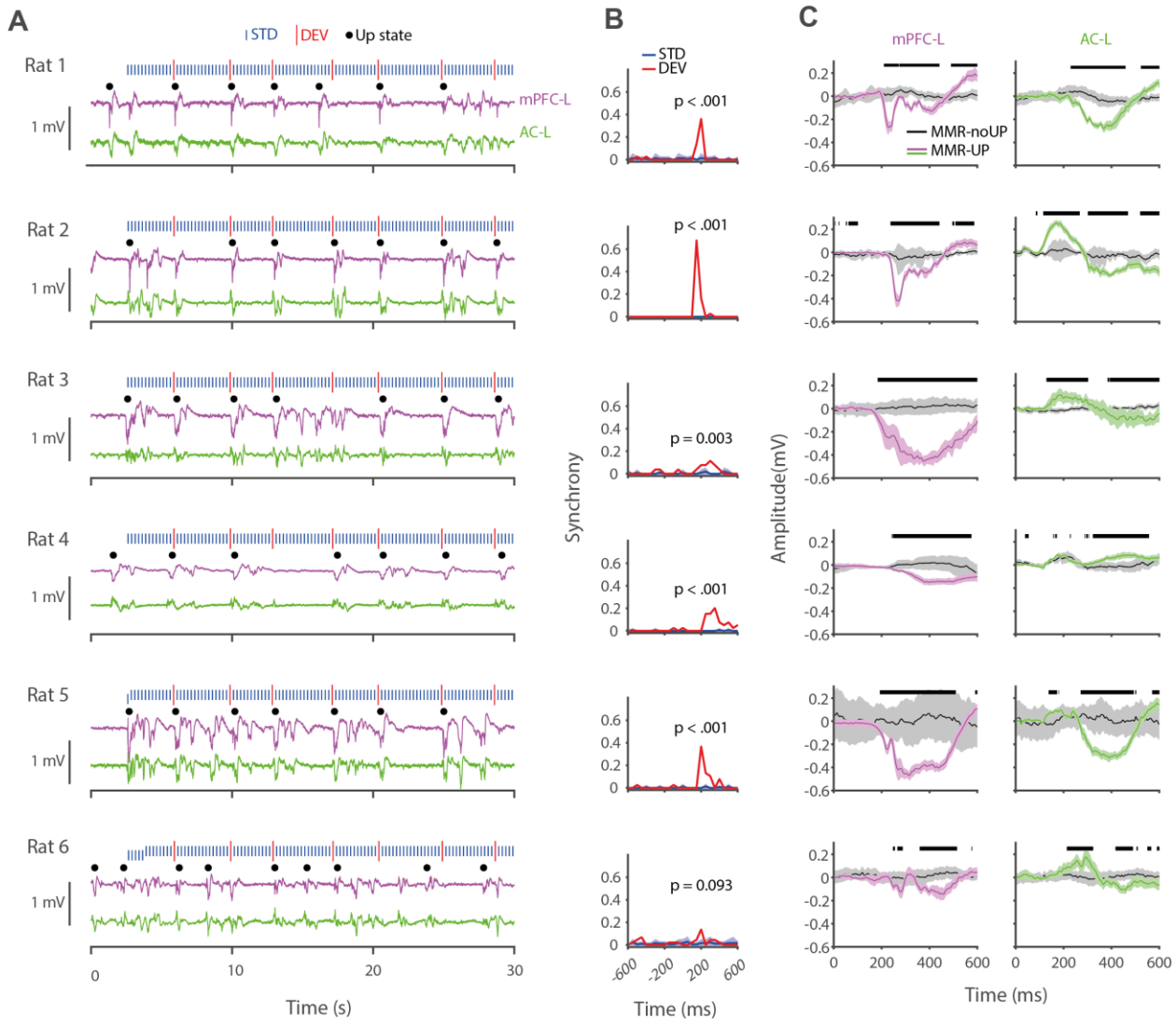

Figure 2: Auditory deviants trigger state initiation producing a mismatch responses. A) LFP traces from the mPFC-L (purple) and AC-L (green), electrode sites 1 and 3, respectively. For animals 1-6 (rows), an oddball paradigm was presented with a SOA of 250 ms and inter-DEV interval of 3 - 4.75 s (11 – 18 STDs (blue bars; pseudorandomised). Auditory DEV (red bar) was often followed by Up phase initiation (black dot). For clarity only the initial 30s are shown, full stimuli length was 620 stimuli, 40 DEVs, 155s. **B)** Cross-correlation synchrony between Up phase initiation and DEV or STD stimuli presentation. Significantly higher synchrony in the DEV condition compared to the STD (Mean ± 95% CI for the STDs 2-5 stimuli before a DEV) condition is observed in all animals with a ~200ms latency, demonstrating reliable initiation of cortical Up phase by the auditory DEV. Two-sample t-tests used for statistical comparison. **C)** MMRs from

151 mPFC-L (left) or AC-L (right) electrode sites, when an Up phase was initiated (purple/green) or
152 not initiated (black). When auditory DEVs triggered Up phases, a MMR was present in both AC-L
153 and mPFC-L. Further, the animals with greatest synchrony between DEV stimuli and Up phase
154 initiation also show the largest amplitude MMR. Black bar marks significance between MMR-
155 noUp and MMR-Up (two-sample t-test). 0ms represents the stimulus onset.

156 **Up phase initiation is the sole deviant response under urethane anesthesia**

157 We then tested a classical oddball paradigm (250 ms SOA; 10% DEV probability; mean inter-DEV
158 interval of 2.5 s; flip-flop design 10/14.142 kHz; 60 dB SPL; 75 ms tones). Using this stimulus
159 paradigm, DEV stimuli triggered cortical Up phases in all animals, however with a lower
160 reliability than in the previous oddball (Fig 3A). Up phases were triggered by 16%, 42%, 13%,
161 35%, 27% and 17% of DEVs in rats 1-6, respectively. We propose this result is due to the shorter
162 inter-DEV interval, which is often too short for cortical neurons to recover from adaptation and
163 return to an excitable state [45]. To study where Up phases are initiated and propagated, we
164 aligned all Up phase responses to the mPFC-L negative peak (Fig 3B). The shortest latency Up
165 phase response was most often in the AC-L, with later responses in the mPFC-L and AC-R. For
166 example, in Rat 2, latencies of the first major peak were AC-L: 169ms, AC-R: 197ms and mPFC-L:
167 271ms. This result is consistent with the Up phase travelling wave beginning in the AC-L as the
168 site of thalamocortical input during the right-sided stimulus presentation. Up phases travel
169 across the cortex at a rate of ~30 mm/s [46,47], producing our later responses in AC-R and mPFC-L.
170 We then studied whether any other responses to DEVs were present or if Up phase triggering
171 was the sole DEV response (Fig 3C). Here we divided the data into 3 categories: 1) Up phases
172 that were initiated by a DEV, 2) spontaneous Up phases, and 3) auditory DEVs that did not
173 induce an Up phase. Comparison of these three responses revealed very similar responses
174 shapes for Up phases that occurred spontaneously and those evoked by a DEV. In comparison,
175 no responses were observed when the DEV failed to evoke an Up phase, consistent with the
176 lack of MMR response in Fig 2C. In our urethane-anesthetised rat preparation, the entire
177 deviant and MMR response is a result of cortical Up phase initiation.
178

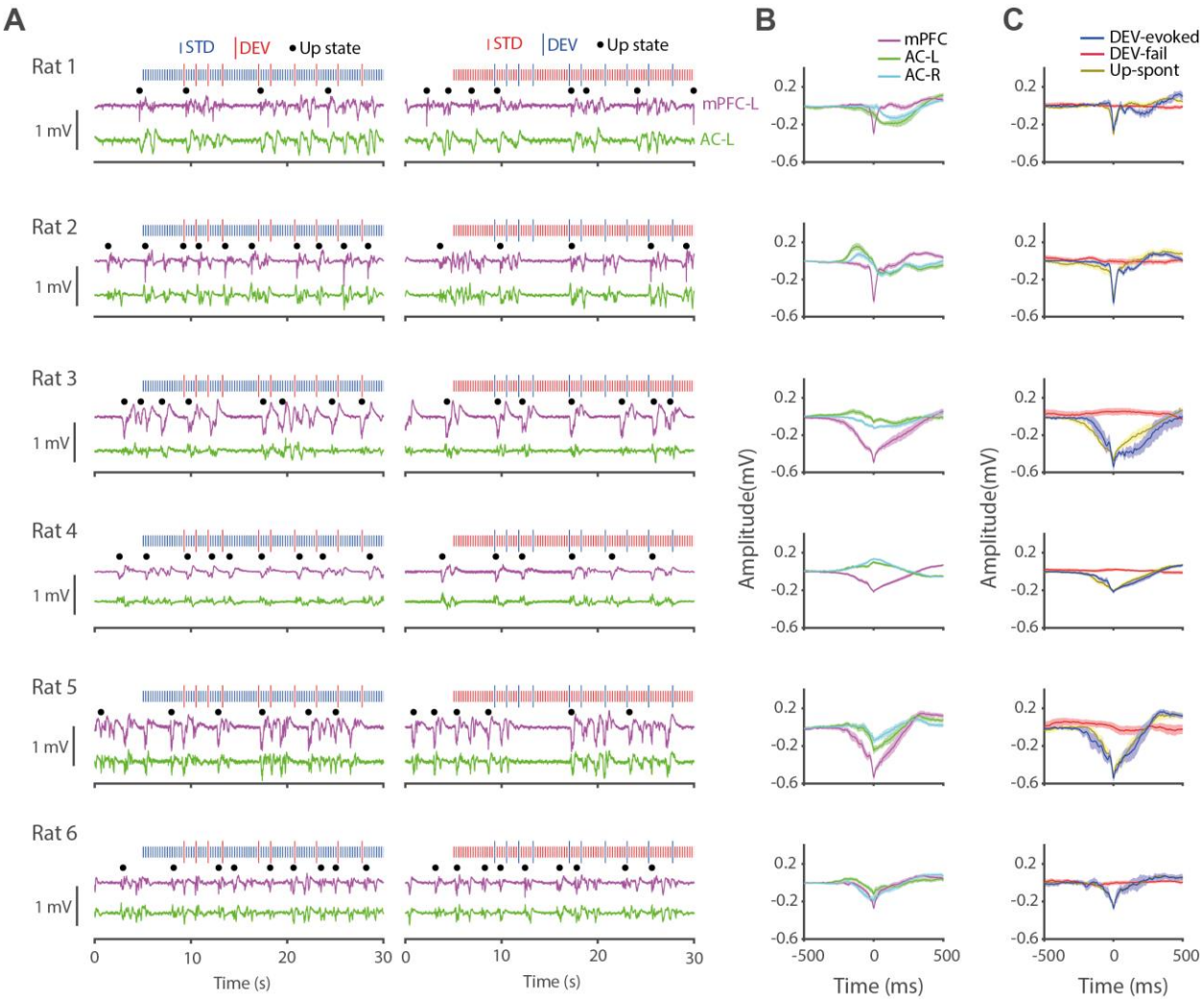

Fig 3. A generic auditory Oddball paradigm also initiates cortical Up phases. A) LFP traces from the mPFC-L (purple) and AC-L (green). For each animal (rows), a classical oddball paradigm was presented with a 250 ms SOA and 10% DEV probability. Black dots mark the timing of Up phase initiations and blue and red bars represent the two frequencies of the auditory oddball paradigm, with the larger bar representing the DEV. For clarity only the initial 30s are shown, full stimuli length was 400 stimuli, 40 DEVs, 100s. **B)** Plots of MMR at different electrode sites mPFC-L, AC-L and AC-R, electrode sites 1, 3 and 5, respectively. Generally, an initial peak is seen in the AC-L, followed by a later peak in the mPFC-L. All peak aligned to Up phase initiation on mPFC-L electrode. **C)** DEV-evoked Up phases (blue) and spontaneous Up phases (yellow) show similar response profiles. In comparison, when DEVs failed to evoke an Up phase (red), no other response is observed.

192 **Omissions do not trigger Up phase initiation**

193 Omitted tones (Omi) in a predictable stimulus sequence can produce prediction error responses
194 in the cortex [48–50], so we hypothesised that Omi stimuli may trigger cortical Up phases. We
195 tested two different Omi paradigms, with either a 250 ms SOA (Rats 3 & 4; 6.45% Omi
196 probability; inter- Omi interval 3 - 4.75 s; STD 10 kHz 60 dB SPL 75 ms) or 125 ms SOA (Rats 5 &
197 6; 6.45% Omi probability; inter-Omi interval 1.5 – 2.375 s; STD 10 kHz 60 dB SPL 75 ms). Omi
198 stimuli were not found to initiate cortical Up phases (Fig 4A). Auditory omissions are capable of
199 initiating prediction error responses in the AC [48–50], but these are generally smaller than the
200 responses to STD stimuli. Hence, they likely are not sufficient to induce an Up phase. The post-
201 Omi stimuli (POST) were able to trigger Up phases in the 250 ms SOA condition, likely due to
202 the period of silence preceding the POST resulting in increased thalamocortical input during the
203 POST stimulus. The latency of Up phase initiation is consistent with being a response to the
204 POST and not to the Omi.
205

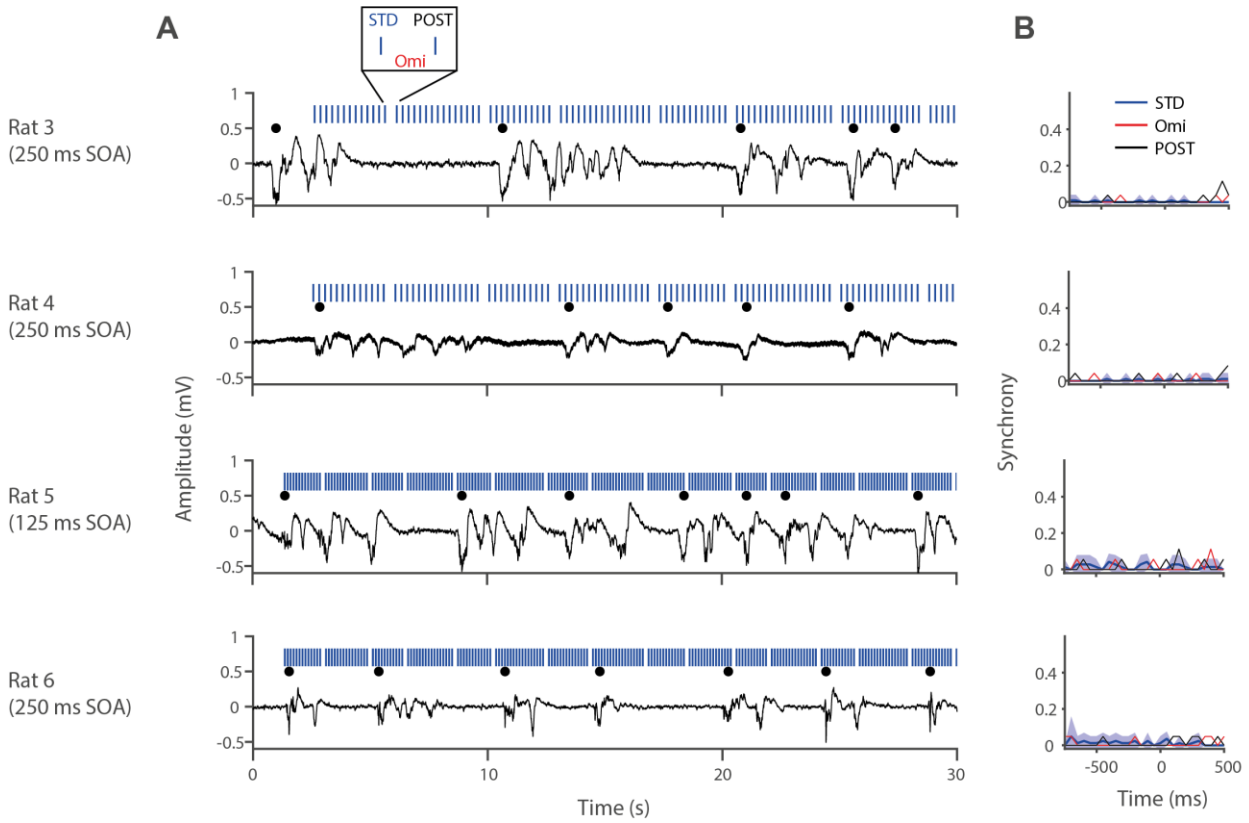

Figure 4: Omissions do not trigger cortical Up phases. A) LFP traces from the mPFC-L. In animals 3-6 (rows), omission paradigms consisting of a repeating STD (blue bars) and Omi (spaces) were tested for Up phase initiation (black dots). Animals 3&4 were tested with a 250 ms SOA, and animals 5&6 a 125 ms SOA. For clarity only the initial 30s are shown, full stimuli length was 620 stimuli, 40 DEVs, 77/155s. **B)** Cross-correlation synchrony between Up phase initiation and Omi or STD stimuli presentation revealed that silent Omi or repeating STD stimuli did not initiate cortical Up phases in any animal. However, the POST stimuli were able to trigger Up phases in the 250 ms SOA condition in Rats 3 & 4 (two-sample t-test, $p = 0.0019$). The latency of Up phase triggering is consistent with Up phase triggering by the POST.

DISCUSSION

We recorded ECoG responses under urethane-anesthesia and found cortical slow oscillations consisting of Up and Down phases (Fig 1). When presenting an auditory oddball paradigm, DEV stimuli triggered cortical Up phase initiation, thus generating a MMR (Fig 2). Further, when a DEV failed to initiate an Up phase, we observed no other DEV response (Fig 3), suggesting that triggering of Up phase initiation is the sole mechanism for MMR generation under urethane anesthesia. Neurons of the auditory thalamus show stimulus-specific adaptation and large

225 responses to DEVs [33,43,44], therefore we propose a potential mechanism for Up phase initiation
226 is through increased thalamocortical activity, as has been previously described in other sensory
227 systems [11–13]. Our data also provide indirect evidence for thalamocortical drive initiating cortical
228 Up phases, however further studies would be warranted involving modulation of the
229 thalamocortical pathway to confirm this.
230 Adaptive and predictive mechanisms that modulate the thalamocortical activity may be key to
231 generating sensory cortex responses to DEVs in unconscious states, which then trigger cortical
232 Up phases, resulting in MMR signals. This proposed mechanism suggests that during the
233 auditory oddball paradigm, a prediction error response to a DEV in the thalamocortical
234 projection can produce a long-latency MMR response throughout the cortex. While these
235 responses are due to a prediction error in the thalamus, they may not be a true prediction error
236 response in all cortical areas, and solely a result of an increased thalamocortical input initiating
237 an Up phase. Further studies measuring cortical Up phases while activating thalamocortical
238 pathways could test the proposed mechanism. If this potential mechanism is accurate, care
239 must be taken when interpreting long-latency PE in the cortex during unconscious states.
240 We did not find triggering of cortical Up phases by Omi stimuli (Fig 4), likely as these do no
241 increase thalamocortical activity sufficiently to trigger an Up phase initiation. Previous LFP
242 studies in animal models have failed to show omission responses, likely because responses are
243 very weak and in a small number of neurons. Only when recording single neurons are responses
244 apparent and present in the cortex [48–50]. Hence these omission responses cannot be attributed
245 to an Up phase initiation. Therefore, cortical Omi responses under urethane anaesthesia likely
246 remain a true prediction error signal.
247 Long-latency responses to auditory deviants during anesthesia synchronized sleep have been
248 described, but have not previously been attributed to state change [51–53]. Our present data
249 demonstrate that the MMR is solely due to a phase change during the desynchronised state of
250 deep anesthesia (comparable to non-rapid eye movement sleep), however the relation of this
251 to MMN when awake is currently unknown. We also observe in Fig 3 that animals in a more
252 synchronised state with stronger Up and Down phases exhibit more reliable Up state triggering
253 by DEVs, indicating that anesthetic depth is likely key to this effect. While more subtle, cortical

254 state changes also occur during wakefulness. Such state changes are dependent on thalamic
255 and basal forebrain input [3,54–56], and are altered by attention [1,2]. The effect of DEVs on cortical
256 state during wakefulness is an intriguing area of study, and may underlie previous models of
257 MMN involving attentional shifting [57,58].
258 The present data show that DEVs trigger cortical Up phase initiation in the urethane-
259 anesthetised rat, producing MMRs. MMRs produced by Up phases occur at the lowest latency
260 in AC then spread to other areas, producing MMN and P300-like responses in the AC and mPFC,
261 respectively. In summary, Up phase initiation is the sole generator of MMRs in the urethane-
262 anesthetised rat.

263 **METHODS**

264 **Ethical approval**

265 All animal experimental procedures were performed under protocols established by the
266 Directive of the European Communities (86/609/CEE, 2003/65/CE, and 2010/63/UE) and
267 RD53/2013 Spanish Legislation for the use and care of animals. All the details of the study were
268 approved by the Bioethics Committee of the University of Salamanca (USAL-ID-887). Female
269 Long-Evans rats were obtained from Janvier Labs (Le Genest-Saint-Isle, France), and
270 experiments were performed on animals weighing 210-280g. Rats were housed on a 12/12 h
271 light-dark cycle, with food and water available *ad libitum*.
272

273 **Anesthetic induction and auditory brainstem responses**

274 All experiments were made inside a chamber with acoustic insulation and electrical protection.
275 Anesthesia was induced with urethane (1.9 g kg^{-1}, i.p.; Sigma-Aldrich, St Louis, U.S.A.), then a
276 further 0.315 - 0.63 g kg^{-1} dose at 45 minutes if required to induce surgical anesthetic depth.
277 This dose is greater than that used previously to induce robust synchronised states consisting of
278 Up and Down states [20]. Corneal and rear paw withdrawal reflexes were routinely monitored.
279 Ophthalmic gel (Lipolasic 2 mg/g; Bausch Lomb, Vaughan, Canada) was applied for avoid dry
280 eyes in the animals. During all experimental procedures, the animals were artificially ventilated
281 through a tracheotomy with O_2, monitoring the CO_2 levels, and temperature was maintained at
282 36 - 38°C using a rectal probe and a homeostatic heating blanket (Cibertec, Madrid, Spain)
283 placed under the animal.
284 Sound stimuli were presented using Tucker-Davis Technologies (TDT; Alachua, FL, USA)
285 hardware and presented monaurally to the right ear through a closed system using a custom-
286 made earphone (calibrated to ensure a flat spectrum; ±2 dB at 0.5 - 44 kHz) coupled to a
287 custom-made cone, as a substitute for traditional ear bars. Initially, ABRs were recorded to
288 check for normal hearing in animals. Three needle electrodes were placed into the skin, one at
289 the dorsal midline close to the neural crest, one behind the left pinna, and one behind the right
290 pinna. ABRs were recorded in response to tone bursts (4, 8, 16 and 32 kHz; 5 ms duration, 1 ms
291 rise/fall times, 21 Hz presentation rate, 512 repetitions in 10 dB steps from 0–80 dB SPL;

292 Tucker-Davis Technologies RZ6 & Medusa 4Z preamp). ABR thresholds were analysed with TDT
293 BioSigRZ and all animals showed thresholds ≤40 dB SPL and were considered normal hearing for
294 the following experiments.
295
296 **Surgery and ECoG array implantation**
297 Following ABRs, dexamethasone (Cortexonavet, 0.25 mg kg^{-1}, i.m.; Syva, León, Spain) and
298 atropine (0.1 mg kg^{-1}, s.c.; Braun, Rubi, Spain) were administered to reduce cerebral oedema
299 and bronchial secretions, respectively. Lidocaine was also injected around the pinna tissue to
300 achieve a higher anaesthetic level in these areas. The ears were prepared by removing pinna
301 cartilage to obtain easier access the ear canal, and a tracheotomy allowed artificial ventilation.
302 The animal was placed in the stereotactic frame with the upper jaw attached to a bite bar and
303 the hollow ear bars into the ear canals. The speaker was placed into the right ear bar, while the
304 hollow left ear bar was filled with plasticine. A midline incision was made along the midline of
305 the head, from 5 mm rostral of bregma to the nuchal ridge, as well as small lateral incisions (~3
306 mm) at each end. Connective tissue was removed and the temporalis muscle moved to allow
307 access to the AC-L & AC-R and mPFC. An electrode array was produced, made of 8 silver wires
308 (0.125 mm diameter; WPI, Sarasota, USA) heated at one end to form a ball, to prevent damage
309 to the dura mater, and attached to a ZCA-EIB16 (TDT, Alachua, USA) ZIF-clip connector board [59].
310 A total of 10 burr holes were drilled for electrode placement and anchor screws, at the
311 locations shown in Fig 1A. Silver ball electrodes were placed in the burr holes on the rostral and
312 caudal AC and mPFC. After electrode insertion, the drill holes were filled with Kwik-Cast silicone
313 sealant (World Precision Instruments, Hitchin, UK) and then the entire array covered with
314 dental acrylic (Duralay; Reliance Dental Manufacturin; Alsip, IL, USA). Finally, skin was sutured
315 around the implant. Animals were not allowed to recover, and first recordings were made
316 approximately 1 hour after the end of the surgery.
317
318 **Neural recording and analysis**
319 Custom MATLAB (Mathworks, Natick, USA) code was used to generate stimuli patterns and
320 control presentation through TDT Synapse software. Stimuli were output from the TDT RZ and

presented through a speaker to the right ear. A TDT ZC16 headstage was used to connect the implanted electrodes to a TDT PZ5 preamp connected to a TDT RZ2 processor. The data were filtered (low-pass 7 kHz) and recorded using TDT Synapse software at a sampling rate of 3 kHz. We analysed the TDT stream data as LFP data using custom Matlab scripts. The stream was downsampled to 763Hz, then filtered using an 8th order bandpass filter (0.1-10 Hz for LFPs; 0.1-150 Hz for oscillation analysis), and Up phase initiation found in LFP traces using the Matlab *findpeaks* function (MinPeakDistance = 382; MinPeakProminence = 0.2 mV). Peaks that had another peak in the preceding 1.5s were removed, as they were later waves of the same Up phase. All further analysis, statistical testing and plotting of all data were performed using custom MATLAB scripts. Cross-correlation synchrony was calculated using a bin size of 50 ms. Total synchrony was quantified as the total synchrony measurement for a 250 ms window centered at the peak synchrony timing. Synchrony measures for were statistically compared using two-sample t-tests, comparing the synchrony of the DEV-Up to the synchrony of the STD-Up for the standards preceding the DEV by 2-5 trials.

336 **REFERENCES**

337 1. Harris, K. D. & Thiele, A. Cortical state and attention. *Nat. Rev. Neurosci.* **12**, 509–523
338 (2011).
339 2. Speed, A., Del Rosario, J., Burgess, C. P. & Haider, B. Cortical State Fluctuations across
340 Layers of V1 during Visual Spatial Perception. *Cell Rep.* **26**, 2868-2874.e3 (2019).
341 3. Poulet, J. F. A. & Petersen, C. C. H. Internal brain state regulates membrane potential
342 synchrony in barrel cortex of behaving mice. *Nature* **454**, 881–885 (2008).
343 4. Adamantidis, A. R., Gutierrez Herrera, C. & Gent, T. C. Oscillating circuitries in the
344 sleeping brain. *Nat. Rev. Neurosci.* **20**, 746–762 (2019).
345 5. Sanchez-Vives, M. V. Origin and dynamics of cortical slow oscillations. *Curr. Opin. Physiol.*
346 **15**, 217–223 (2020).
347 6. Neske, G. T. The slow oscillation in cortical and thalamic networks: Mechanisms and
348 functions. *Front. Neural Circuits* **9**, 1–25 (2016).
349 7. Steriade, M., Nuñez, A. & Amzica, F. A novel slow (<1 Hz) oscillation of neocortical
350 neurons in vivo: Depolarizing and hyperpolarizing components. *J. Neurosci.* **13**, 3252–
351 3265 (1993).
352 8. Steriade, M., Nuñez, A. & Amzica, F. Intracellular analysis of relations between the slow
353 (<1 Hz) neocortical oscillation and other sleep rhythms of the electroencephalogram. *J.*
354 *Neurosci.* **13**, 3266–3283 (1993).
355 9. Maria V. Sanchez-Vives & David A. McCormick. Cellular and network mechanisms of
356 rhythmic recurrent activity in neocortex Maria. *Nat. Neurosci.* **3**, 1027–1034 (2000).
357 10. Timofeev, I., Grenier, F., Bazhenov, M., Sejnowski, T. J. & Steriade, M. Origin of slow
358 cortical oscillations in deafferented cortical slabs. *Cereb. Cortex* **10**, 1185–1199 (2000).
359 11. David, F. *et al.* Essential thalamic contribution to slow waves of natural sleep. *J. Neurosci.*
360 **33**, 19599–19610 (2013).
361 12. Rigas, P. & Castro-Alamancos, M. A. Thalamocortical up states: Differential effects of
362 intrinsic and extrinsic cortical inputs on persistent activity. *J. Neurosci.* **27**, 4261–4272
363 (2007).
364 13. Lemieux, M., Chen, J. Y., Lonjers, P., Bazhenov, M. & Timofeev, I. The impact of cortical

365 deafferentation on the neocortical slow oscillation. *J. Neurosci.* **34**, 5689–5703 (2014).
366 14. Contreras, D. & Steriade, M. Cellular Basis of EEG Slow Rhythms: A Study of Dynamic
367 Corticothalamic Relationships. *J. Neurosci.* **15**, 604–622 (1995).
368 15. Hasenstaub, A., Sachdev, R. N. S. & McCormick, D. A. State changes rapidly modulate
369 cortical neuronal responsiveness. *J. Neurosci.* **27**, 9607–9622 (2007).
370 16. Ji, D. & Wilson, M. A. Coordinated memory replay in the visual cortex and hippocampus
371 during sleep. *Nat. Neurosci.* **10**, 100–107 (2007).
372 17. Petersen, C. C. H., Hahn, T. T. G., Mehta, M., Grinvald, A. & Sakmann, B. Interaction of
373 sensory responses with spontaneous depolarization in layer 2/3 barrel cortex. *Proc. Natl.*
374 *Acad. Sci. U. S. A.* **100**, 13638–13643 (2003).
375 18. Pagliardini, S., Gosgnach, S. & Dickson, C. T. Spontaneous Sleep-Like Brain State
376 Alternations and Breathing Characteristics in Urethane Anesthetized Mice. *PLoS One* **8**,
377 1–10 (2013).
378 19. Mondino, A. *et al.* Urethane anaesthesia exhibits neurophysiological correlates of
379 unconsciousness and is distinct from sleep. *Eur. J. Neurosci.* **59**, 483–501 (2024).
380 20. Clement, E. A. *et al.* Cyclic and sleep-like spontaneous alternations of brain state under
381 urethane anaesthesia. *PLoS One* **3**, (2008).
382 21. Gretenkord, S., Rees, A., Whittington, M. A., Gartside, S. E. & Lebeau, F. E. N. Dorsal vs.
383 ventral differences in fast Up-state-associated oscillations in the medial prefrontal cortex
384 of the urethane-anesthetized rat. *J. Neurophysiol.* **117**, 1126–1142 (2017).
385 22. Gretenkord, S. *et al.* Electrical stimulation of the ventral tegmental area evokes sleep-like
386 state transitions under urethane anaesthesia in the rat medial prefrontal cortex via
387 dopamine D1-like receptors. *Eur. J. Neurosci.* **52**, 2915–2930 (2020).
388 23. Durán, E., Yang, M., Neves, R., Logothetis, N. K. & Eschenko, O. Modulation of Prefrontal
389 Cortex Slow Oscillations by Phasic Activation of the Locus Coeruleus. *Neuroscience* **453**,
390 268–279 (2021).
391 24. Jercog, D. *et al.* UP-DOWN cortical dynamics reflect state transitions in a bistable
392 network. *Elife* **6**, 1–33 (2017).
393 25. Sterzer, P. *et al.* The Predictive Coding Account of Psychosis. *Biol. Psychiatry* **84**, 634–643

394 (2018).
395 26. Sapey-Triomphe, L. A., Pattyn, L., Weilnhammer, V., Sterzer, P. & Wagemans, J. Neural
396 correlates of hierarchical predictive processes in autistic adults. *Nat. Commun.* **14**,
397 (2023).
398 27. Kocagoncu, E., Klimovich-Gray, A., Hughes, L. E. & Rowe, J. B. Evidence and implications
399 of abnormal predictive coding in dementia. *Brain* **144**, 3311–3321 (2021).
400 28. Lee, M. *et al.* Neural mechanisms of mismatch negativity dysfunction in schizophrenia.
401 *Mol. Psychiatry* **22**, 1585–1593 (2017).
402 29. Ross, J. M. & Hamm, J. P. An expanding repertoire of circuit mechanisms for visual
403 prediction errors. *Trends Neurosci.* **xx**, 1–2 (2024).
404 30. Garrido, M. I., Kilner, J. M., Stephan, K. E. & Friston, K. J. The mismatch negativity: A
405 review of underlying mechanisms. *Clin. Neurophysiol.* **120**, 453–463 (2009).
406 31. Malmierca, M. S., Carbajal, G. V. & Escera, C. *Deviance Detection and Encoding Acoustic*
407 *Regularity in the Auditory Midbrain*. *The Oxford Handbook of the Auditory Brainstem*
408 (2019). doi:10.1093/oxfordhb/9780190849061.013.19.
409 32. Fitzgerald, K. & Todd, J. Making Sense of Mismatch Negativity. *Front. Psychiatry* **11**, 1–19
410 (2020).
411 33. Parras, G. G. *et al.* Neurons along the auditory pathway exhibit a hierarchical
412 organization of prediction error. *Nat. Commun.* **8**, (2017).
413 34. Strauss, M. *et al.* Disruption of hierarchical predictive coding during sleep. *Proc. Natl.*
414 *Acad. Sci. U. S. A.* **112**, E1353–E1362 (2015).
415 35. Nashida, T. *et al.* Automatic auditory information processing in sleep. *Sleep* **23**, 821–828
416 (2000).
417 36. Sallinen, M., Kaartinen, J. & Lyytinen, H. Is the appearance of mismatch negativity during
418 stage 2 sleep related to the elicitation of K-complex? *Electroencephalogr. Clin.*
419 *Neurophysiol.* **91**, 140–148 (1994).
420 37. Quaedflieg, C. W., Münte, S., Kalso, E. & Sambeth, A. Effects of remifentanil on
421 processing of auditory stimuli: A combined MEG/EEG study. *J. Psychopharmacol.* **28**, 39–
422 48 (2014).

423 38. Koelsch, S., Heinke, W., Sammler, D. & Olthoff, D. Auditory processing during deep
424 propofol sedation and recovery from unconsciousness. *Clin. Neurophysiol.* **117**, 1746–
425 1759 (2006).
426 39. Malmierca, M. S., Cristaudo, S., Pérez-González, D. & Covey, E. Stimulus-specific
427 adaptation in the inferior colliculus of the anesthetized rat. *J. Neurosci.* **29**, 5483–5493
428 (2009).
429 40. Ayala, Y. A. & Malmierca, M. S. Cholinergic modulation of stimulus-specific adaptation in
430 the inferior colliculus. *J. Neurosci.* **35**, 12261–12272 (2015).
431 41. Taaseh, N., Yaron, A. & Nelken, I. Stimulus-specific adaptation and deviance detection in
432 the rat auditory cortex. *PLoS One* **6**, (2011).
433 42. Polterovich, A., Jankowski, M. M. & Nelken, I. Deviance sensitivity in the auditory cortex
434 of freely moving rats. *PLoS One* **13**, 3–8 (2018).
435 43. Antunes, F. M., Nelken, I., Covey, E. & Malmierca, M. S. Stimulus-specific adaptation in
436 the auditory thalamus of the anesthetized rat. *PLoS One* **5**, (2010).
437 44. Valerio, P., Rechenmann, J., Joshi, S., De Franceschi, G. & Barkat, T. R. Sequential
438 maturation of stimulus-specific adaptation in the mouse lemniscal auditory system. *Sci.*
439 *Adv.* **10**, 1–16 (2024).
440 45. Compte, A., Sanchez-Vives, M. V., McCormick, D. A. & Wang, X. J. Cellular and network
441 mechanisms of slow oscillatory activity (<1 Hz) and wave propagations in a cortical
442 network model. *J. Neurophysiol.* **89**, 2707–2725 (2003).
443 46. Stroh, A. *et al.* Making Waves: Initiation and Propagation of Corticothalamic Ca2+ Waves
444 In Vivo. *Neuron* **77**, 1136–1150 (2013).
445 47. Ruiz-Mejias, M., Ciria-Suarez, L., Mattia, M. & Sanchez-Vives, M. V. Slow and fast rhythms
446 generated in the cerebral cortex of the anesthetized mouse. *J. Neurophysiol.* **106**, 2910–
447 2921 (2011).
448 48. Lao-Rodríguez, A. B. *et al.* Neuronal responses to omitted tones in the auditory brain: A
449 neuronal correlate for predictive coding. *Sci. Adv.* (2023) doi:10.1126/sciadv.abq8657.
450 49. Awwad, B., Jankowski, M. M., Polterovich, A., Bashari, S. & Nelken, I. Extensive
451 representation of sensory deviance in the responses to auditory gaps in unanesthetized

452 rats. *Curr. Biol.* **33**, 3024-3030.e3 (2023).
453 50. Auksztulewicz, R., Rajendran, V. G., Peng, F., Schnupp, J. W. H. & Harper, N. S. Omission
454 responses in local field potentials in rat auditory cortex. *BMC Biol.* **21**, 1–16 (2023).
455 51. Loewy, D. H., Campbell, K. B., De Lugt, D. R., Elton, M. & Kok, A. The mismatch negativity
456 during natural sleep: Intensity deviants. *Clin. Neurophysiol.* **111**, 863–872 (2000).
457 52. Casado-Román, L., Carbajal, G. V., Pérez-González, D. & Malmierca, M. S. Prediction error
458 signaling explains neuronal mismatch responses in the medial prefrontal cortex. *PLoS*
459 *Biol.* **18**, 1–29 (2020).
460 53. Xiong, Y. (Sophy) *et al.* Propofol- mediated loss of consciousness disrupts predictive
461 routing and local field phase modulation of neural activity. *Proc. Natl. Acad. Sci.* **121**,
462 (2024).
463 54. Poulet, J. F. A. & Crochet, S. The cortical states of wakefulness. *Front. Syst. Neurosci.* **12**,
464 1–18 (2019).
465 55. Crochet, S. & Petersen, C. C. H. Correlating whisker behavior with membrane potential in
466 barrel cortex of awake mice. *Nat. Neurosci.* **9**, 608–610 (2006).
467 56. Greenberg, D. S., Houweling, A. R. & Kerr, J. N. D. Population imaging of ongoing
468 neuronal activity in the visual cortex of awake rats. *Nat. Neurosci.* **11**, 749–751 (2008).
469 57. Escera, C., Yago, E., Corral, M. J., Corbera, S. & Nuñez, M. I. Attention capture by auditory
470 significant stimuli: Semantic analysis follows attention switching. *Eur. J. Neurosci.* **18**,
471 2408–2412 (2003).
472 58. Escera, C. Neural Mechanisms of Involuntary Attention to Acoustic Novelty and Change.
473 *J. Cogn. Neurosci.* **10**, 590–604 (1990).
474 59. Berger, J. I. *et al.* Gap-induced reductions of evoked potentials in the auditory cortex: A
475 possible objective marker for the presence of tinnitus in animals. *Brain Res.* **1679**, (2018).

476